Assessing vegetation response to drought in the Laohahe catchment, North China

Xiaofan Liu, Liliang Ren, Fei Yuan, Jing Xu and Wei Liu

ABSTRACT

In order to better understand the relationship between vegetation vigour and moisture availability, a correlation analysis based on different vegetation types was conducted between time series of monthly Normalized Difference Vegetation Index (NDVI) and Palmer Drought Severity Index (PDSI) during the growing season from April to October within the Laohahe catchment. It was found that NDVI had good correlation with PDSI, especially for shrub and grass. The correlation between NDVI and PDSI varies significantly from one month to another. The highest value of correlation coefficients appears in June when the vegetation is growing; lower correlations are noted at the end of growing season for all vegetation types. The influence of meteorological drought on vegetation vigour is stronger in the first half of the growing season, before the vegetation reaches the peak greenness. In order to take the seasonal effect into consideration, a regression model with seasonal dummy variables was used to simulate the relationship between NDVI and PDSI. The results showed that the NDVI–PDSI relationship is significant ($\alpha = 0.05$) within the growing season, and that NDVI is an effective indicator to monitor and detect droughts if seasonal timing is taken into account.

Key words | correlation analysis, drought, NDVI, Palmer drought severity index, regression analysis

Xiaofan Liu
Liliang Ren (corresponding author)
Fei Yuan
State Key Laboratory of Hydrology,
Water Resources and Hydraulic Engineering,
College of Hydrology and Water Resources,
Hohai University,
No. 1 Xikang Road, Nanjing 210098,
China
E-mail: RLL@hhu.edu.cn

Xiaofan Liu
Sichuan Communication Surveying & Design
    Institute,
No. 35 Taishengbei Road, Chengdu 610017,
China

Jing Xu
Department of Hydrosciences,
Nanjing University,
No. 22 Hankou Road, Nanjing 210093,
China

Wei Liu
Shandong Hydrology and Water Resources Survey
    Bureau,
No. 127 Lishan Road, Jinan 250013,
China

INTRODUCTION

Drought is a complex natural hazard that causes economic, environmental and social consequences worldwide. Global economic loss caused by drought each year is up to 6–8 billion US dollars, which is much more than other natural hazards (Wilhite 2000). In the agricultural sector, drought is one of the dominant causes of crop loss in China. According to statistics, the mean annual area of drought was about 21.6 million hectares during the period 1949–1999, accounting for 60% of the total area of meteorological disasters, and crop loss was about 10 billion kilograms in each year (Yuan & Zhou 2004).

It is difficult to detect and monitor drought for three reasons: (1) it develops slowly, and the onset and end are indistinct; (2) it is not precisely and universally defined; and (3) its impact is non-structural and often spread over very large areas (Wilhite 2000; Lei & Albert 2003). The complex drought phenomenon can be represented by a drought index, which allows scientists to quantify climate anomalies in terms of intensity, duration and spatial extent. In China, some widely used drought indices include the Palmer Drought Severity Index (PDSI) (Palmer 1965), the surface humid index (Ma & Fu 2001), the Standardized Precipitation Index (SPI) (Mckee et al. 1993) and the Water Deficit Index (WDI) (Moran et al. 1994).

Palmer (1965) developed the PDSI according to the concept that it is climatically appropriate for existing condition (CAFEC), which carried the drought index research a step forward. The effects of water deficit and duration on drought severity are considered by the PDSI comprehensively. The main items of water budget in the PDSI include precipitation, evapotranspiration runoff and soil water content, which can be calculated by the water balance method or a hydrological model. In addition, the influence of water deficit in the prior period on drought

in the later period is also considered by the PDSI. All of these characteristics mean that the PDSI has explicit physical meanings and spatial and temporal comparability. Since the theory, advantages and calculation method of the PDSI were introduced by Fan & Zheng (1984), Chinese meteorologists have modified the PDSI model using local meteorological data in order to establish the meteorological drought model of China (An & Xing 1986; Liu *et al.* 2004). Nowadays, the PDSI is widely used to represent the genesis, severity, onset, end and duration of drought in China (Wei *et al.* 2003).

In addition to drought indices, satellite sensor data have been playing an increasingly important role in monitoring drought-related vegetation conditions. The National Oceanic and Atmospheric Administration (NOAA) Advanced Very High Resolution Radiometer (AVHRR) is the most widely applied spaceborne sensor for investigating droughts. The sensor has been orbiting the globe since the late 1970s with five spectral channels (one in the visible, one in the near infrared, one in the mid-infrared and two in the thermal range; Bayarjargal *et al.* 2006). The Normalized Difference Vegetation Index (NDVI) derived from AVHRR data has been widely used to monitor and evaluate terrestrial vegetation vigour.

Because the NDVI is highly correlated to green-leaf density and vigour, it is considered to be a proxy for the status of above-ground biomass at the landscape level and is widely used in remote sensing of the terrestrial environment (Bannari *et al.* 1995; Lei & Albert 2003). The close relationship between vegetation vigour and available soil moisture, especially in arid and semi-arid areas, means that the AVHRR-derived NDVI has been used to evaluate drought condition by directly comparing it to precipitation or drought indices (Tucker 1989; Gutman 1990).

Although a number of previous studies have indicated a strong relationship between AVHRR-NDVI and precipitation, air temperature or Standard Precipitation Index (SPI; Li *et al.* 2002; Lei & Albert 2003; Wang *et al.* 2003; Liu & Xu 2007), this relationship is far more complex than what can be represented by simple linear correlation between two variables. It has been noted that the impact of water availability on vegetation changes considerably within different phenological periods of the vegetation growth cycle. It is necessary to take seasonality into account in the understanding of vegetation vigour and drought index relationships. This study therefore attempts to demonstrate a statistical method that considers the seasonal timing effects of moisture availability.

Drought has often threatened the subsistence environment in northern China, resulting in water resources scarcity, environment degradation and desertification. The objective of this paper is to assess the influence of drought on vegetation vigour in northern China by analysis of monthly AVHRR-NDVI and PDSI relationships. In order to take the seasonal effect into consideration, a regression model with seasonal dummy variables was used to simulate the relationship between the NDVI and PDSI for different vegetation types.

STUDY AREA AND DATA PREPARATION

Study area

The Laohahe catchment is located in the semi-arid region of northern China and has a drainage area of 18,599 km², with the Xiaoheyan hydrological station (42°26′ N, 119°34′ E) at the catchment outlet (Figure 1). Elevation within the catchment ranges from 444 to 1,836 m above mean sea level, with elevation declining from the southwest towards the northeast. Forest, shrub, grass and croplands make up most of the vegetation cover in the Laohahe catchment. There are 52 rain gauges and four meteorological stations in this basin (Figure 1) and the recorded data are available from 1960 to 2005. Average annual maximum (minimum) temperature is 14 °C (2 °C) ranging from −4 (−16) in January to 29 (18) in July. The average annual precipitation is approximately 451 mm, and the spatial and temporal distribution of precipitation is uneven. About 88% of the annual precipitation occurs during the months from May through September.

Data preparation

The digital elevation model (DEM) data within 40.9–42.9 °N and 117.2–120 °E at the spatial resolution of 30 × 30 s were
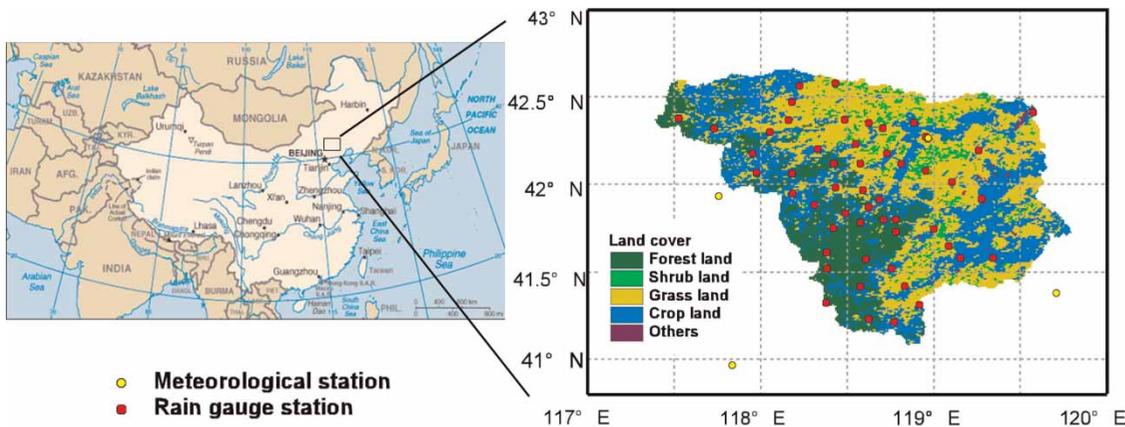
Figure 1 │ Location of the Laohahe catchment and distribution of land cover, meteorological stations and rain gauge stations within the catchment.

obtained from the Global Land 1-km Base Elevation database. The river network and catchment boundary were automatically generated by the digital elevation drainage network model (Martz & Garbrecht 1992).

The University of Maryland's 1 km global land cover data were used to represent the vegetation cover over the study area. The main vegetation types in the study area include forest, shrub, grass and crop, the area percentages of which are 18.1, 5.6, 40.2 and 35.6%, respectively (Figure 1).

The NOAA-AVHRR NDVI dataset is available monthly for the globe at an interval of 8 km, covering the period from July 1981 to September 2001. The basin part of NDVI was clipped using the basin boundary and transferred into the geography projection and the resolution of 30 s in Arc/Info software.

The required meteorological data include daily mean, maximum and minimum air temperature, air vapour pressure, wind velocity, daylight duration and precipitation. In this study, daily precipitation data were obtained from 52 rainfall gauge stations spread across the catchment, and other meteorological data were obtained from four meteorological stations around the catchment. Based on the DEM, the key meteorological variables were topographically corrected with the empirical relationships extracted from data for the entire Laohahe catchment (Ren *et al.* 2009). All meteorological data were interpolated over the whole study area using the inverse distance square method (Ashraf *et al.* 1997).

METHODOLOGY

Computation of PDSI

Monthly PDSI values have been calculated for each grid cell at a spatial resolution of 30 s over the Laohahe catchment using the meteorological data (see above) for the period 1960–2005. PDSI is standardized for different regions and time periods, which is useful in common assessment for a wide area with different climate. The basic concepts and computation steps are as follows (Szep *et al.* 2005).

Step 1. Several methods can generally be used to calculate the potential evapotranspiration, a key variable of the water balance and also of the PDSI computation procedure (Thornthwaite 1948; Liu *et al.* 2004). In this study, the Penman–Monteith equation is applied:

$$ET_0 = \frac{0.408\Delta(R_n - G) + \gamma(900/(T + 273))U_2(e_s - e_a)}{\Delta + \gamma(1 + 0.34U_2)} \quad (1)$$

where ET_0 is the reference evapotranspiration (mm d^{-1}); R_n is the net radiation absorbed by land surface (MJ m^{-2} d^{-1}); G is the soil heat flux (MJ m^{-2} d^{-1}); T is daily mean temperature ($^{\circ}$C); e_s and e_a are the saturation and actual vapour pressures (kPa), respectively; U_2 is the wind speed (m s^{-1}) at 2 m height; γ is the psychrometric constant (kPa $^{\circ}$C^{-1}); and Δ is the first-order derivative of saturation vapour pressure with temperature (kPa $^{\circ}$C^{-1}).

Step 2. After daily potential evapotranspiration has been calculated using the Penman–Monteith equation, monthly potential evapotranspiration and monthly precipitation are calculated using daily data. A simple water balance model was used to calculate the hydrological variables in the PDSI model. The soil was divided into two arbitrary layers: the upper layer was assumed to contain 40 mm of available moisture at field capacity and the lower layer 200 mm (Liu *et al.* 2004). The loss from the underlying layer depends on the initial moisture content, as well as on the computed potential evapotranspiration (PE) and the available water capacity (AWC) of the soil system. Runoff is assumed to occur if and only if both layers reach their combined moisture capacity, AWC. In addition to PE, three more potential terms were used and defined as follows: potential recharge (PR) is the amount of moisture required to bring the soil to its water-holding capacity; potential loss (PL) is the amount of moisture that could be lost from the soil by evapotranspiration during a zero precipitation period; and potential runoff (PRO) is defined as the difference between precipitation and potential recharge.

Step 3. Climatic coefficients were estimated by simulating the water balance for the period of available weather records. Monthly climate coefficients were computed as proportions between climatic averages of actual versus potential values of evaporation, recharge, runoff and loss, respectively.

Step 4. Coefficients were used to determine the amount of precipitation (I) required for the CAFEC, i.e. 'normal' weather during each individual month.

Step 5. The difference between the actual precipitation (P) and CAFEC precipitation (I) is an indicator of water deficiency or surplus in that month, expressed as $D = P - I$. These departures are converted into indices of moisture anomaly as $Z = K \times D$, where K is a weighting factor, which also accounts for spatial variability of the departures D.

Step 6. In the final step the Z-index time series are analyzed to develop criteria for the beginning and ending of drought periods and an empirical formula for determining drought severity. In this study, the empirical formula is (Liu *et al.* 2004):

$$X_i = 0.9331X_{i-1} + Z_i/125.99 \tag{2}$$

where Z_i is the moisture anomaly index and X_i is the PDSI

for the ith month. The equation indicates that PDSI of a given month strongly depends on its value in the previous months and on the moisture anomaly of the actual month.

Time series of monthly NDVI and PDSI

Based on the grid cell at a spatial resolution of 30 s, the monthly NDVI and PDSI of all grid cells in each vegetation cover type within the study area were determined. The time series of monthly NDVI and PDSI for each vegetation type were calculated by averaging the values of the grid cells with the same vegetation type. Only data acquired during the growing season (April–October) were used for the analysis.

Correlation and regression analysis

Pearson correlation and linear regression analyses were conducted for the NDVI versus PDSI. Because the relationship between vegetation vigour and water availability varies within a growing season, each month was analyzed separately. The correlation coefficients and their *p*-values were obtained. The *p*-value of the correlation coefficient is the probability of rejecting the null hypothesis that there is no correlation between two variables.

Because the linear relationships between NDVI and PDSI are significantly different for different seasonal periods, seasonal dummy variables were employed in the regression model (Doran 1989). In this study, the dummy variables were a set of six levels assigned to the 6 months of the growing season and used to account for the effect of the month on NDVI. The regression model containing seasonal dummy variables is expressed as:

$$\begin{aligned} \text{NDVI} = {} & \beta_0 + \beta_1(\text{PDSI}) + \beta_2 D_1 + \beta_3 D_2 + \beta_4 D_3 \\ & + \beta_5 D_4 + \beta_6 D_5 + \beta_7 D_6 + \beta_8 D_1(\text{PDSI}) + \beta_9 D_2(\text{PDSI}) \\ & + \beta_{10} D_3(\text{PDSI}) + \beta_{11} D_4(\text{PDSI}) + \beta_{12} D_5(\text{PDSI}) \\ & + \beta_{13} D_6(\text{PDSI}) + \varepsilon \end{aligned} \tag{3}$$

where $D_1, D_2, \ldots, D_6$ are the dummy variables; $\beta_0, \beta_1, \ldots, \beta_{13}$ are the regression coefficients, and ε is random error. Table 1 lists the assigned binary values of dummy variables $D_1, D_2, \ldots, D_6$.

Table 1 │ Binary value of dummy variables

Month	D_1	D_2	D_3	D_4	D_5	D_6
April	0	0	0	0	0	0
May	1	0	0	0	0	0
June	0	1	0	0	0	0
July	0	0	1	0	0	0
August	0	0	0	1	0	0
September	0	0	0	0	1	0
October	0	0	0	0	0	1

Useful variables were selected by eliminating non-significant variables with large *p*-values step by step (Lei & Albert 2003). The coefficient of determination R^2 was used to measure goodness-of-fit of the model, or closeness of the relationship between the NDVI and PDSI. In the study, $\alpha = 0.05$ was used as the cutoff for rejection of the null hypothesis for all the statistical tests.

RESULTS AND DISCUSSION

Covariation of NDVI and PDSI time series

The relationship between vegetation vigour and moisture availability was clarified by analyzing the covariation of NDVI and PDSI time series with the scatter plots and Pearson correlation analysis. Scatter plots and correlation coefficients of the NDVI and PDSI for different vegetation types during the growing season months can be seen in Figure 2.

It can be noted that the correlation coefficients vary by month and vegetation type. For example, in September and October there are no significant correlations between the NDVI and PDSI, while significant correlations are found for the other months in the growing season for every vegetation type. Very high positive correlations between the NDVI and PDSI for all vegetation types appear in June when the vegetation is growing, but not in August when the vegetation has reached the peak greenness. Lower correlations are noted at the end of growing season for all vegetation types. This situation implies that the influence of drought on vegetation vigour is stronger in the first half

of the growing season before the vegetation reaches the peak greenness, after which the influence of drought on vegetation vigour is quickly weakened.

The correlation coefficients between the NDVI and PDSI for shrub and grass are higher during the growing season, lowest for forest and moderate for crops. This finding indicates that the influence of drought on shrub and grass is stronger while forest has lesser response to droughts in the Laohahe catchment. The different influences of drought on vegetation depend on two factors: (1) the plant growing environment; and (2) vegetation characteristics. The forest is mostly distributed in the upstream high elevation region within the Laohahe catchment, where precipitation is relatively abundant. Precipitation is not the dominant factor which restricts the growth of plant in such region, thus the influence of drought on forest is less. The root depths of shrub and grass are shallow, and therefore sensitive to precipitation. They are therefore more responsive to droughts.

Seasonal timing of vegetation and moisture relationship

The correlation analyses demonstrate that the relationship between the NDVI and PDSI varies markedly during the growing season (Figure 2). The examples discussed above indicate that there is a stronger relationship in the first half of the growing season (April–August) than at the end (September–October). The correlations between the NDVI and PDSI for all vegetation types are shown in Figure 3. The seasonal vegetation growth characteristics, e.g. onset, peak and senescence, can be easily seen on these graphs. When comparing the correlation coefficients with the NDVI phenological cycle, it is clear that vegetation response to moisture availability varies significantly between months.

The seasonal patterns of NDVI for all vegetation types are unimodal, with the maximum values appearing in August. The highest significant correlations between the NDVI and PDSI occur in June when the vegetation is growing, while lower correlations appear during senescence (Figure 3). This analysis of the correlation between the NDVI and PDSI indicates that vegetation response to drought depends on the plant growth stage. Salter & Goode (1967) defined the 'moisture-sensitive period' to
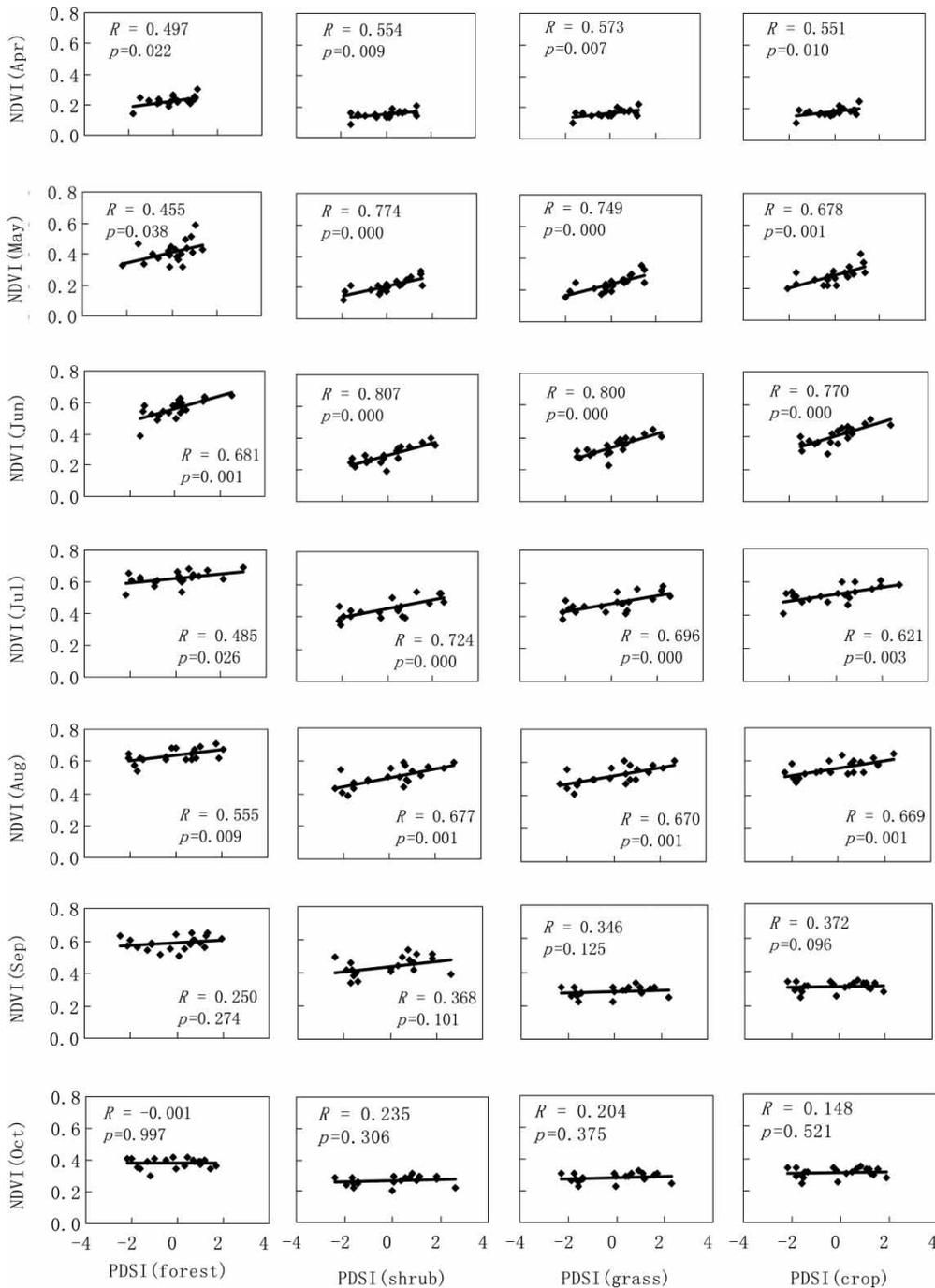
Figure 2 | Scatter plots and correlation coefficients of the NDVI and PDSI for different vegetation types within the Laohahe catchment. Values in plots represent correlation coefficients (*R*) and *p*-values.

imply a particular period during the development of a plant in which the plant is more sensitive to moisture condition. In general, the moisture-sensitive period occurs during the development of reproductive organs, when plants obtain maximum beneficial effect from the available water supply. During this period, drought has the greatest effect on reducing plant size and yield. Consequently, irrigation has the greatest effect on increasing yield, and excess water has
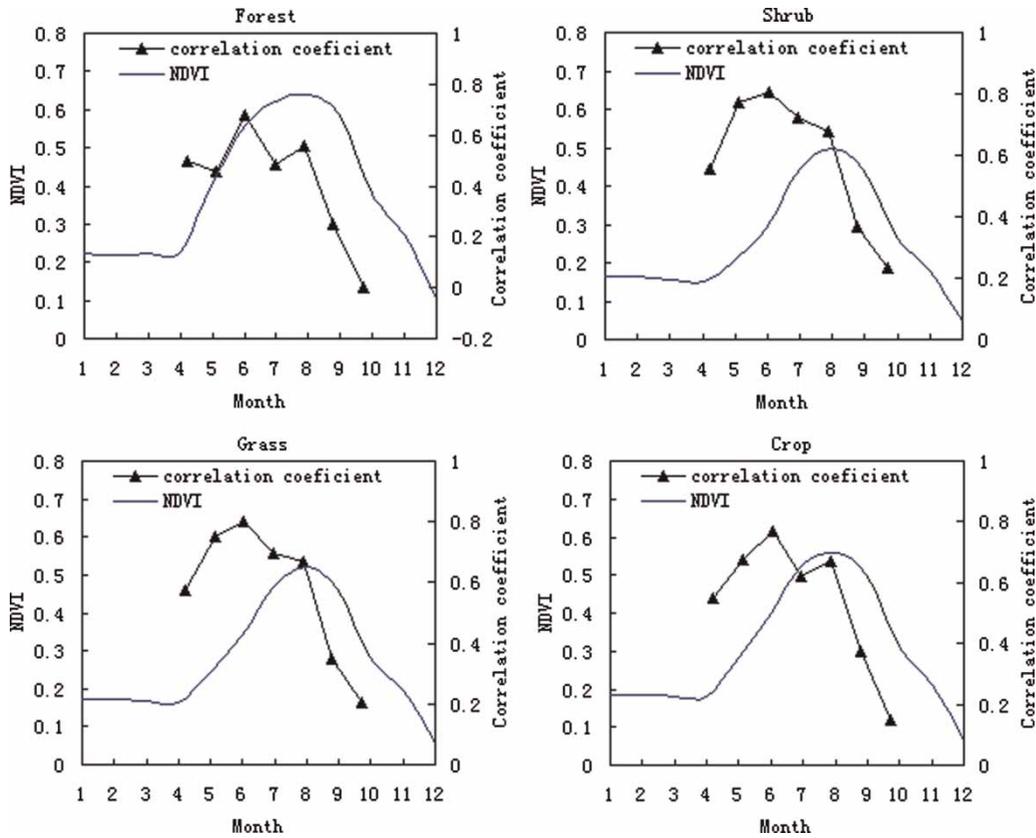
Figure 3 │ Seasonal change of correlation coefficient of the NDVI and PDSI, with comparison with seasonal NDVI variations for all vegetation types. The NDVI curves were obtained by averaging monthly values over all 21 years.

the smallest adverse effect on yield in the period (Lei & Albert 2003). In this study, the highest correlations appear in June when the vegetation is growing, which is the moisture-sensitive period for the vegetations in the Laohahe catchment.

Relationship between NDVI and PDSI

The goodness-of-fit of the NDVI and PDSI correlation was tested and measured using analysis of variance and R^2 from the regression model with dummy variables (Equation (3)). Tables 2–5 show the results of the regression models for forest, shrub, grass and croplands, respectively. Based on the regression models with dummy variables, the correlations between the NDVI and PDSI for all vegetation types are very significant, with *p*-value <0.001 and $R^2 > 0.9$. The useful variables were retained in the model, after non-significant items were eliminated.

Table 2 │ Regression analysis on the NDVI and PDSI for forest land in Laohahe catchment

Variable	Coefficient	Standard error	t-value	p-value
Intercept	0.2266	0.009	25.292	<0.0001
PDSI	0.0112	0.003	3.346	0.0011
D_1	0.1845	0.013	14.563	<0.0001
D_2	0.3304	0.013	26.079	<0.0001
D_3	0.3955	0.013	31.224	<0.0001
D_4	0.4121	0.013	32.53	<0.0001
D_5	0.3613	0.013	28.513	<0.0001
D_6	0.1555	0.013	12.268	<0.0001
D_1 (PDSI)	0.0228	0.011	2.101	0.0374
D_2 (PDSI)	0.0303	0.01	3.049	0.0027

$F_{9,137} = 199.593$, *p*-value < 0.001, $R^2 = 0.929$, $R^2_{adj} = 0.924$.

The following regression functions representing the linear relationship between the NDVI and PDSI for forest in each month of the growing season were obtained by

Table 3 | Regression analysis on the NDVI and PDSI for shrub land in Laohahe catchment

Variable	Coefficient	Standard error	t-value	p-value
Intercept	0.1503	0.008	18.718	<0.0001
PDSI	0.0099	0.004	2.734	0.0071
D_1	0.0571	0.011	5.026	<0.0001
D_2	0.1422	0.011	12.521	<0.0001
D_3	0.2952	0.011	25.997	<0.0001
D_4	0.3485	0.011	30.699	<0.0001
D_5	0.2901	0.011	25.548	<0.0001
D_6	0.1149	0.011	10.117	<0.0001
D_1 (PDSI)	0.0235	0.009	2.67	0.0085
D_2 (PDSI)	0.0297	0.008	3.527	0.0006
D_3 (PDSI)	0.0173	0.006	2.692	0.0079
D_4 (PDSI)	0.0173	0.006	2.662	0.0087

$F_{11,135} = 159.37$, p-value < 0.001, $R^2 = 0.928$, $R^2_{adj} = 0.923$.

Table 4 | Regression analysis on the NDVI and PDSI for grassland in Laohahe catchment

Variable	Coefficient	Standard error	t-value	p-value
Intercept	0.1632	0.008	20.612	<0.0001
PDSI	0.0095	0.004	2.552	0.0118
D_1	0.0755	0.011	6.736	<0.0001
D_2	0.1734	0.011	15.481	<0.0001
D_3	0.3116	0.011	27.827	<0.0001
D_4	0.3572	0.011	31.899	<0.0001
D_5	0.298	0.011	26.606	<0.0001
D_6	0.1214	0.011	10.833	<0.0001
D_1 (PDSI)	0.0279	0.009	3.118	0.0022
D_2 (PDSI)	0.0331	0.009	3.881	0.0002
D_3 (PDSI)	0.0154	0.007	2.367	0.0193
D_4 (PDSI)	0.0154	0.007	2.313	0.0221

$F_{11,135} = 165.64$, p-value < 0.001, $R^2 = 0.931$, $R^2_{adj} = 0.925$.

inserting the estimated coefficients (Table 2) and the values of dummy variables into Equation (3):

$$\text{April NDVI} = 0.2266 + 0.0112(\text{PDSI}) \tag{4a}$$

$$\text{May NDVI} = 0.4111 + 0.034(\text{PDSI}) \tag{4b}$$

$$\text{June NDVI} = 0.557 + 0.0415(\text{PDSI}) \tag{4c}$$

Table 5 | Regression analysis on the NDVI and PDSI for cropland in Laohahe catchment

Variable	Coefficient	Standard error	t-value	p-value
Intercept	0.1812	0.008	22.969	0.0000
PDSI	0.0184	0.003	5.937	0.0000
D_1	0.1014	0.011	9.085	0.0000
D_2	0.2203	0.011	19.742	0.0000
D_3	0.3465	0.011	31.057	0.0000
D_4	0.3798	0.011	34.044	0.0000
D_5	0.3193	0.011	28.61	0.0000
D_6	0.1297	0.011	11.576	0.0000
D_1 (PDSI)	0.0196	0.009	2.201	0.0293
D_2 (PDSI)	0.0243	0.008	2.896	0.0044
D_6 (PDSI)	−0.0151	0.007	-2.224	0.0277

$F_{10,136} = 202.819$, p-value < 0.001, $R^2 = 0.937$, $R^2_{adj} = 0.933$.

$$\text{July NDVI} = 0.6221 + 0.0112(\text{PDSI}) \tag{4d}$$

$$\text{August NDVI} = 0.638 + 0.0112(\text{PDSI}) \tag{4e}$$

$$\text{September NDVI} = 0.5879 + 0.0112(\text{PDSI}) \tag{4f}$$

$$\text{October NDVI} = 0.3821 + 0.0112(\text{PDSI}) \tag{4g}$$

The following regression functions representing the linear relationship between the NDVI and PDSI for shrubland in each month of the growing season were obtained by inserting the estimated coefficients (Table 3) and the values of dummy variables into Equation (3):

$$\text{April NDVI} = 0.1503 + 0.0099(\text{PDSI}) \tag{5a}$$

$$\text{May NDVI} = 0.2074 + 0.0334(\text{PDSI}) \tag{5b}$$

$$\text{June NDVI} = 0.2925 + 0.0396(\text{PDSI}) \tag{5c}$$

$$\text{July NDVI} = 0.4455 + 0.0272(\text{PDSI}) \tag{5d}$$

$$\text{August NDVI} = 0.4988 + 0.0272(\text{PDSI}) \tag{5e}$$

$$\text{September NDVI} = 0.4404 + 0.0099(\text{PDSI}) \tag{5f}$$

$$\text{October NDVI} = 0.2652 + 0.0099(\text{PDSI}) \qquad (5\text{g})$$

The following regression functions representing the linear relationship between the NDVI and PDSI for grassland in each month of the growing season were obtained by inserting the estimated coefficients (Table 4) and the values of dummy variables into Equation (3):

$$\text{April NDVI} = 0.1632 + 0.0095(\text{PDSI}) \qquad (6\text{a})$$

$$\text{May NDVI} = 0.2387 + 0.0374(\text{PDSI}) \qquad (6\text{b})$$

$$\text{June NDVI} = 0.3366 + 0.0426(\text{PDSI}) \qquad (6\text{c})$$

$$\text{July NDVI} = 0.4748 + 0.0249(\text{PDSI}) \qquad (6\text{d})$$

$$\text{August NDVI} = 0.5204 + 0.0249(\text{PDSI}) \qquad (6\text{e})$$

$$\text{Septmber NDVI} = 0.4612 + 0.0095(\text{PDSI}) \qquad (6\text{f})$$

$$\text{October NDVI} = 0.2846 + 0.0095(\text{PDSI}) \qquad (6\text{g})$$

The following regression functions representing the linear relationship between the NDVI and PDSI for cropland in each month of growing season were obtained by inserting the estimated coefficients (Table 5) and the values of dummy variables into Equation (3):

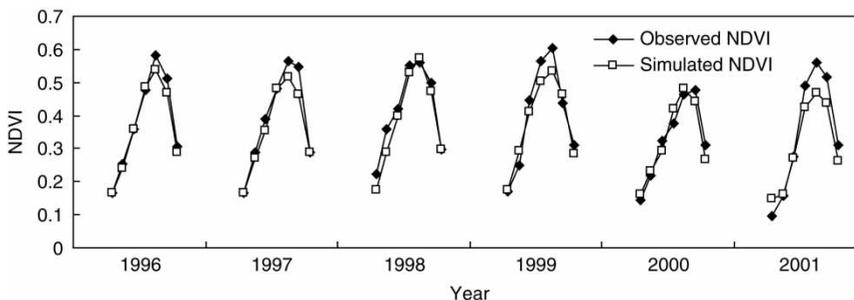$$\text{April NDVI} = 0.1812 + 0.0184(\text{PDSI}) \qquad (7\text{a})$$

$$\text{May NDVI} = 0.2826 + 0.038(\text{PDSI}) \qquad (7\text{b})$$

$$\text{June NDVI} = 0.4015 + 0.0427(\text{PDSI}) \qquad (7\text{c})$$

$$\text{July NDVI} = 0.5277 + 0.0184(\text{PDSI}) \qquad (7\text{d})$$

$$\text{August NDVI} = 0.561 + 0.0184(\text{PDSI}) \qquad (7\text{e})$$

$$\text{September NDVI} = 0.5005 + 0.0184(\text{PDSI}) \qquad (7\text{f})$$

$$\text{October NDVI} = 0.3109 + 0.0033(\text{PDSI}) \qquad (7\text{g})$$

The different intercepts and slopes of these regression equations indicate the change of the NDVI-PDSI relationships from one month to another. The maximum values of intercepts are in August for all vegetation types, as a result of the maximum values of NDVI occurring in August. The maximum values of slopes of all vegetation types appear in June, which highlights the fact that vegetation is most sensitive to moisture conditions in June.

The relationship between the NDVI and PDSI can be simulated by the regression model with dummy variables. Taking grassland for example, the monthly NDVI of grass during the period 1996–2001 was simulated. Figure 4 shows the comparison between the simulated and observed NDVI for the grassland during the growing season from 1996 to 2001. The simulated NDVI using the regression with dummy variables fits the observed NDVI quite well, and the regression model with dummy variables has a very high goodness-of-fit.

Figure 4 | Comparison between the simulated and observed NDVI for the grassland in the Laohahe catchment.

CONCLUSIONS

The purpose of this paper was to assess vegetation response to drought within the Laohahe catchment by analysis of monthly AVHRR-NDVI and PDSI relationships based on vegetation types of forest, shrub, grass and crop. The correlation coefficients between NDVI and PDSI vary by month. Very high positive correlations between the NDVI and PDSI for all vegetation types appear in June when the vegetation is growing, and the lower correlations are noted at the end of the growing season. This situation implies that the influence of drought on vegetation vigour is stronger in the first half of the growing season before the vegetation reaches its peak greenness, after which the influence of drought on vegetation vigour is quickly weakened. The relationship between NDVI and PDSI is also affected by vegetation type. The correlation coefficients for shrub and grass are higher during the growing season, while the correlation coefficient for forest is lowest among the main vegetation types. This finding can be interpreted in terms of growing environment and plant root-depth characteristics.

When comparing the correlation coefficients with the NDVI phenological cycle, it is clear that vegetation response to moisture availability varies significantly between months. This analysis of the correlation between the NDVI and PDSI indicates that vegetation response to drought depends on the plant growth stage. In the Laohahe catchment, June is the moisture-sensitive period for vegetations. During this period, drought has the greatest effect on the vegetation growth.

When regression techniques are used to quantify the relationship between the NDVI and PDSI, the seasonal effect was taken into account. The good goodness-of-fit of the NDVI and PDSI correlation using a regression model with dummy variables illustrated that the NDVI is a good indicator of moisture condition and can be an important data source when used for detecting and monitoring drought in this area. Furthermore, it demonstrates that seasonality is an important factor when NDVI and NDVI-derived vegetation indices are used for drought detection.

ACKNOWLEDGEMENTS

REFERENCES

An, S. & Xing, J. 1986 A modified Palmer's drought index. *Journal of Academy of Meteorological Science, China* **1** (1), 75–82.

Ashraf, M., Loftis, J. & Hubbard, K. G. 1997 Application of geostatistics to evaluate partial weather station networks. *Agricultural and Forest Meteorology* **84**, 255–271.

Bannari, A., Morin, D. & Bonn, F. 1995 A review of vegetation indices. *Remote Sensing Reviews* **13**, 95–120.

Bayarjargal, Y., Karnieli, A., Bayasgalan, M., Khudulmur, S., Gandush, C. & Tucker, C. J. 2006 A comparative study of NOAA-AVHRR derived drought indices using change vector analysis. *Remote Sensing of Environment* **105**, 9–22.

Doran, H. 1989 *Applied Regression Analysis in Econometrics*. Marcel Dekker, New York.

Fan, J. & Zheng, J. 1984 The introduction of Palmer meteorological drought research method. *Meteorology Technology* **1**, 63–71.

Gutman, G. G. 1990 Towards monitoring drought from space. *Journal of Climate* **3**, 282–295.

Lei, J. & Albert, J. P. 2003 Assessing vegetation response to drought in the northern Great Plains using vegetation and drought indices. *Remote Sensing of Environment* **87**, 85–98.

Li, B., Tao, S. & Dawson, R. W. 2002 Relation between AVHRR NDVI and ecoclimatic parameters in China. *International Journal of Remote Sensing* **22**, 989–999.

Liu, L. & Xu, H. 2007 Change of NDVI of main vegetations and their relationship with meteorological factors in Yellow River Basin. *Chinese Journal of Agrometeorology* **28** (3), 334–337.

Liu, W., An, S., Liu, G. & Guo, A. 2004 The farther modification of Palmer drought severity model. *Journal of Applied Meteorological Science* **15** (2), 207–216.

Ma, Z. & Fu, C. 2001 Trend of surface humid index in the arid area of northern China. *Acta Meteorological Sinica* **59** (6), 737–746.

Martz, W. & Garbrecht, J. 1992 Numerical definition of drainage network and subcatchment areas from digital elevation models. *Computers and Geotechics* **18** (6), 747–761.

Mckee, T. B., Doesken, N. J. & Kleist, J. 1993 The relationship of drought frequency and duration to time scales. In *Proceedings of the Eighth Conference on Applied Climatology*, Boston, MA. American Meteorological Society, pp. 179–184.

Moran, M. S., Clarke, T. R., Inoue, Y. & Vidal, A. 1994 Estimating crop water deficit using the relation between surface-air

temperature and spectral vegetation index. *Remote Sensing of Environment* **49**, 246–263.

Palmer, W. C. 1965 *Meteorological Drought*. US Department of Commerce, Weather Bureau Research Paper, No. 45, Washington, DC.

Ren, L., Liu, X., Yuan, F., Singh, V. P., Fang, X., Yu, Z. & Zhang, W. 2009 Quantitative effect of land use and land cover change on green water and blue water in northern part of China. In: *Hydrological Changes and Watershed Management from Headwaters to the Ocean* (M. Taniguchi, W. C. Burnett, Y. Fukushima, M. Haigh & Y. Umezawa, eds.), Taylor & Francis Group, London, pp. 187–193.

Salter, P. J. & Goode, J. E. 1967 *Crop Responses to Water at Different Stages of Growth*. Commonwealth Agricultural Bureaux, Farnham Royal, Bucks, England.

Szep, I., Mika, J. & Dunkel, Z. 2005 Palmer drought severity index as soil moisture indicator: physical interpretation, statistical behaviour and relation to

global climate. *Physics and Chemistry of the Earth* **30**, 231–243.

Thornthwaite, C. W. 1948 An approach towards a rational classification of climate. *Geographical Reviews* **38**, 55–94.

Tucker, C. J. 1989 Comparing SMMR and AVHRR data for drought monitoring. *International Journal of Remote Sensing* **10**, 1663–1672.

Wang, J., Rich, P. M. & Price, K. P. 2003 Temporal response of NDVI to precipitation and temperature in the central Great Plains, USA. *International Journal of Remote Sensing* **24**, 2345–3364.

Wei, J., Tao, S. & Zhang, Q. 2003 Analysis of drought in Northern China based on the Palmer severity drought index. *Acta Geographica Sinica* **58** (Supplement), 91–99.

Wilhite, D. A. 2000 Drought as a natural hazard. In: *Drought. A Global Assessment, Vol. I* (D. A. Wilhite, ed.). Routledge, London.

Yuan, W. & Zhou, G. 2004 Theoretical study and research prospect on drought indices. *Advances in Earth Science* **19** (6), 982–991.